PERGAMON

Engineering Fracture Mechanics 64 (1999) 649–673

Engineering Fracture Mechanics

www.elsevier.com/locate/engfracmech

The effect of hydrogen on dislocation dynamics

I.M. Robertson*

Department of Materials Science and Engineering, University of Illinois, 1304 W. Green St, Urbana, IL 61801, USA

Abstract

Deformation studies in numerous materials have been performed in situ in a transmission electron microscope equipped with an environmental cell to elucidate the mechanisms of hydrogen embrittlement. The primary results from these studies are that solute hydrogen can increase the velocity of dislocations, increase the crack propagation rate, decrease the stacking-fault energy of 310s stainless steel and increase the propensity for edge character dislocations. Evidence from bulk mechanical property tests to support these results is also discussed.

Keywords: Environmental cell transmission electron microscopy; Hydrogen embrittlement; Dislocations; Hydrogen-enhanced localized plasticity

1. Introduction

The deleterious effect of hydrogen on mechanical properties was first documented in 1875 by Johnson [1], who reported that hydrogen in iron and steels causes a reduction in ductility and fracture stress. Since then it has been shown that hydrogen embrittlement is not restricted to iron and steel but occurs in many materials. In addition to causing a reduction in ductility and fracture stress, it has been shown that hydrogen can cause the fracture mode to change from ductile transgranular to transgranular cleavage or brittle intergranular failure, increase or decrease the flow stress, increase slip localization, and increase slip planarity. In Nb, V, Zr, Ti, and alloys based on them, the presence of hydrogen can result in the formation of a brittle hydride phase. Numerous mechanisms have been proposed to explain the effect of hydrogen on the mechanical properties of materials and it is unlikely that a single mechanism is capable of

* Tel.: +1-217-333-1441; fax: +1-217-333-2736.
E-mail address: ianr@uxl.cso.uiuc.edu (I.M. Robertson).

0013-7944/99/$ - see front matter
PII: S0013-7944(99)00094-6

explaining all effects. The most commonly cited mechanisms include the hydrogen pressure buildup mechanism [2], in which the pressure of hydrogen in bubbles provides the stress for the formation and propagation of a crack; hydrogen adsorption at the crack tip or surface imperfections [3–5], which reduces the surface energy for crack propagation; hydrogen reduction of the cohesive strength of the lattice [6,7]; hydrogen accumulation at precipitates and second-phase particles, which can lead to dislocation generation or nucleation and growth of a crack [8–10]; formation and fracture of a brittle hydride [11]; hydrogen-induced reduction in the stacking-fault energy [12,13]; and hydrogen enhancement of the dislocation mobility, which allows dislocations to move at a lower applied stress [14–16].

In this paper, the discussion is limited to hydrogen effects on dislocation dynamics. Discussion of the other mechanisms can be found elsewhere [17–20].

2. Hydrogen enhanced plasticity mechanism

Beachem [14], based on observations of tear ridges and dimples on fracture surfaces of hydrogen embrittled steels, Fig. 1, suggested that the effect of hydrogen was to "unlock" rather than "lock" dislocations. That is "it [hydrogen] allows them [dislocations] to multiply or move at reduced stresses". Beachem's model was, until the late 1970s, basically ignored by the scientific community despite evidence on fracture surfaces for ductile processes occurring during hydrogen embrittlement. In interpreting such observations it was generally concluded that while plastic deformation had occurred, it was not influenced in any way by solute hydrogen, and was a consequence of the effect of hydrogen on another property. The concept

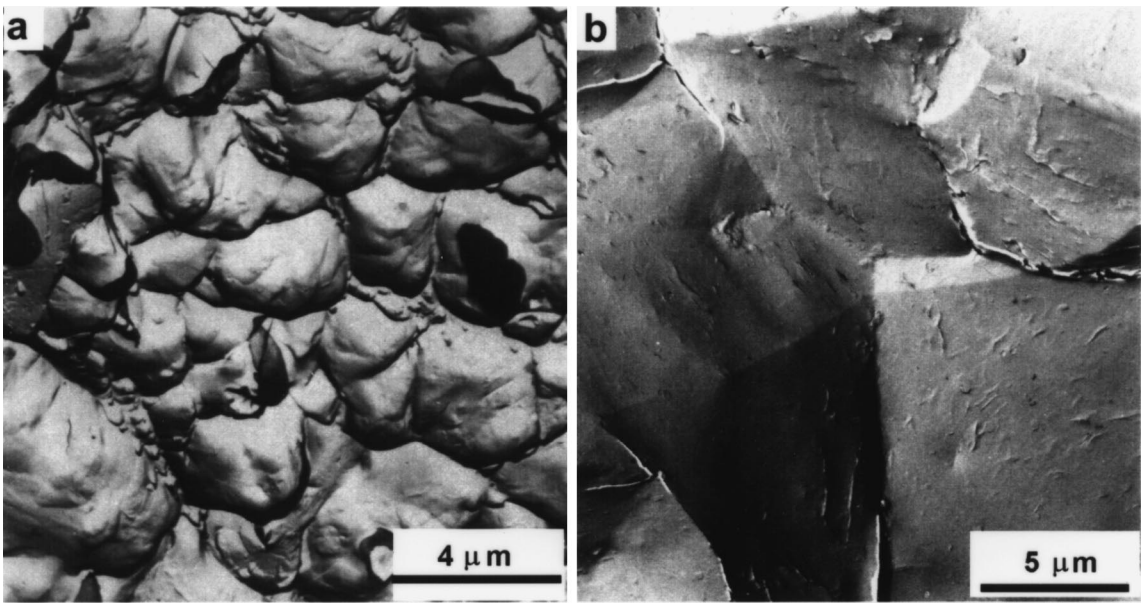

Fig. 1. Replicas showing (a) tear ridges and (b) dimples on a fracture surface of hydrogen embrittled steels [14].

of hydrogen influencing the mobility of dislocations was reintroduced by Lynch [15,21], and by Birnbaum, Robertson and coworkers [22–34].

Lynch [15,21] compared the "brittle" intergranular and transgranular cleavage-like fracture surfaces in nickel specimens tested in liquid metal and in gaseous hydrogen environments. The fracture surfaces of the liquid-metal and gaseous hydrogen embrittled surfaces showed evidence of slip, dimples and tear ridges. These features are all evidence of dislocation activity and led Lynch to propose that crack growth occurred by localized plastic flow in both hydrogen and liquid metal embrittlement. Hydrogen embrittlement, like liquid metal embrittlement, was attributed to the chemisorption of the embrittling element (hydrogen) at the crack tip weakening the interatomic bonds, which facilitated the nucleation and emission of dislocations from the crack tip. In this model, crack advance in vacuum occurred not by the emission of dislocations from the crack tip but by dislocations from the bulk moving to and being absorbed at the crack tip.

To explain the effect of hydrogen on dislocation mobility Sirois and Birnbaum [35] and Birnbaum and Sofronis [36] proposed a different mechanism in which hydrogen formed an atmosphere around dislocations and other elastic stress centers. The redistribution of the hydrogen atmospheres as the stress-fields merge effectively shields the dislocation from the elastic center, reducing the interaction energy between the dislocation and the obstacle. Consequently, dislocations can move at lower levels of applied stress.

Sofronis and Birnbaum [36] have calculated, by using linear elasticity theory and finite element techniques, the effect of a hydrogen atmosphere on the interaction energy between edge dislocations of the same Burgers vector and between an edge dislocation and a solute atom. In considering the formation of H atmospheres around dislocations, they considered two elastic interactions, a first-order interaction associated with introducing a hydrogen atom in the stress field of a defect and a second-order interaction that results from the change in local elastic moduli caused by solute hydrogen. The interaction energy of the first-order interaction, $W_{\mathrm{int}}^{(1)}$, can be expressed as

$$W_{\mathrm{int}}^{1} = \sigma_{ij}^{\mathrm{disl}} \epsilon_{ij}^{\mathrm{H}} \tag{1}$$

where $\sigma_{ij}^{\mathrm{disl}}$ represents the stress field of the dislocation and $\epsilon_{ij}^{\mathrm{H}}$ the strain field of the hydrogen solute. The interaction energy varies as $1/r$, where r is the distance from the dislocation. The interaction energy $W_{\mathrm{int}}^{(2)}$ due to the change in the local moduli can be expressed as

$$W_{\mathrm{int}}^{(2)} = \left(\frac{1}{2}\right) \epsilon_{ij}^{\mathrm{disl}} \epsilon_{kl}^{\mathrm{disl}} V_{\mathrm{H}} (C'_{ijkl} - C_{ijkl}) \tag{2}$$

where $\epsilon_{ij}^{\mathrm{disl}}$ and $\epsilon_{kl}^{\mathrm{disl}}$ are the dislocation strain components, V_{H} is the volume over which the hydrogen solute changes the elastic moduli, and C'_{ijkl} and C_{ijkl} are the elastic stiffness coefficients in the presence and absence of hydrogen, respectively. This second-order interaction varies as $1/r^2$, and can lead to a weak, short-range hydrogen atmosphere if $(C'_{ijkl} - C_{ijkl}) < 0$ or a short-range depletion of hydrogen if $(C'_{ijkl} - C_{ijkl}) > 0$. In an isotropic material, the second-order interaction appears through the dependence of the shear and bulk modulus on the solute concentration. The first order interaction will dominate solute interactions with edge

dislocations, whereas the second-order interaction describes the interaction of solutes with an isotropic distortion field and a screw dislocation.

Assuming that the elastic moduli are unaffected by hydrogen, the redistribution of hydrogen atmospheres around two edge dislocations on the same slip plane and with the same Burgers vector is as shown in Fig. 2. As a result of the linear superposition of the stress fields of the dislocations the distribution of hydrogen around the dislocations changes as they move closer together. The effect of this hydrogen redistribution on the shear stress experienced by one dislocation due to the presence of the other is shown in Fig. 3. With increasing hydrogen concentration, the shear stress experienced by one dislocation due to the other decreases. Consequently, the effect of hydrogen is to reduce the applied stress necessary to move an edge dislocation with a hydrogen atmosphere through a field of elastic obstacles. Similar results, albeit at a reduced level, were obtained when stress relaxations and moduli changes due to the introduction of hydrogen in the dislocation stress field were accounted for in the calculations.

These calculations show that the hydrogen-induced elastic shielding causes a short-range decrease in the elastic force between a dislocation and an obstacle. The magnitude of the effect decreases with increasing distance between the dislocation and the obstacle, and increases with

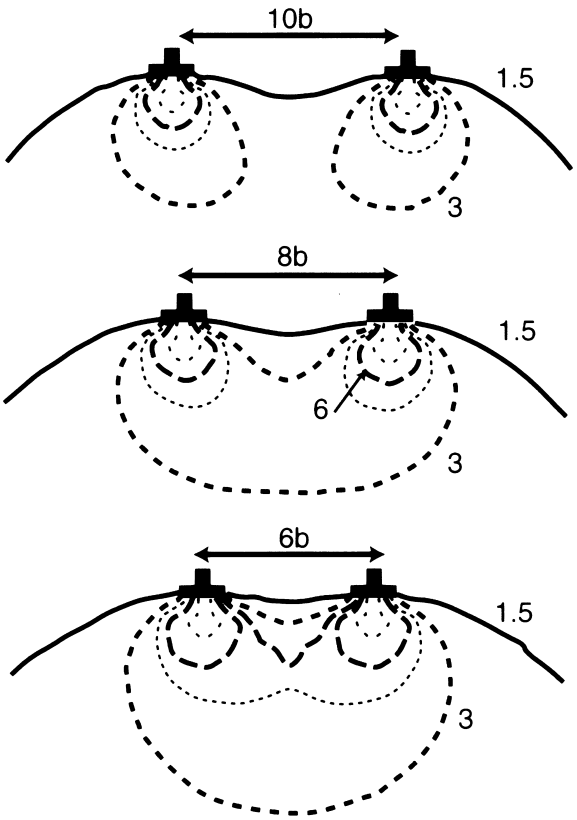

Fig. 2. Changes in the hydrogen isoconcentration lines around two edge dislocations on the same slip plane and with the same Burgers vector as a function of separation distance [36].

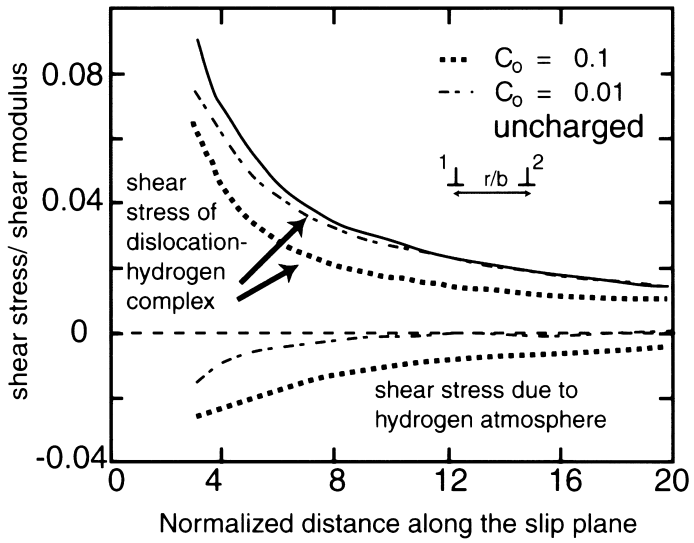

Fig. 3. Effect of the redistribution of hydrogen on the shear stress experienced by one edge dislocation due to the presence of the other. Both dislocations are on the same slip plane [36].

increasing hydrogen concentration. Sofronis and Birnbaum calculated that for a H/M concentration of 0.01, the force between two edge dislocations separated by a distance of $3b$ decreases by about 8%. Increasing the hydrogen concentration to H/M = 0.1 results in a decrease of 21%.

This hydrogen shielding effect is not restricted to the surface, as in Lynch's mechanism, but can occur in the bulk of the material. In the following sections, evidence supporting hydrogen enhancing the generation and mobility of dislocations through the hydrogen-shielding mechanism is presented. Observations from deformation experiments performed in-situ in a transmission electron microscope (TEM) equipped with an environmental cell are presented in section 3. These experiments are, by necessity, performed in thin foils (< 200 nm thick) in which plane stress conditions prevail. However, there is now considerable evidence from tests using thick samples that show hydrogen enhancing the mobility of dislocations and these are described in section 4.

3. Deformation experiments in-situ in an environmental cell transmission electron microscope

Before presenting the observations from the deformation experiments in the environmental cell transmission electron microscope, the microscope and the sample geometry used in these experiments are briefly described.

To be able to perform TEM experiments in a controlled gaseous environment, and maintain operation of the microscope, a method has to be developed to confine the gas in the sample region and to minimize the electron path length in the gas. Electron transparent windows or small apertures, placed either on a specially designed sample holder or in the objective pole-

piece, are used for gas confinement; for details see Ref. [37]. The facilities used in the experiments described below were the HVEM-environmental cell at Argonne National Laboratory and the JEOL 4000 environmental cell microscope at the University of Illinois [38–40]. In both facilities, the objective pole-piece contains a differentially pumped double-aperture cell, which encloses the sample rod and allows a gaseous environment to be maintained around the sample. The gas pressure as measured by an external gauge is much lower than the fugacity at the sample because of dissociation and ionization of the gas molecules by the electron beam. Bond et al. [41] determined that the hydrogen fugacity was between 10^3 and 10^5 times greater than the measured cell pressure. Dynamic effects associated with introducing hydrogen gas into the environmental cell and, hence, to the sample are recorded on videotape via a Gatan TV-rate camera. Although a number of gases have been introduced into the environmental cell, hydrogen gas (or water-saturated gas) is the only one to cause the effects described below.

The type of straining stage used in these experiments is shown in Fig. 4, and the tip region at higher magnification in the inset. The sample is mounted to the movable drawbar by placing the sample over the posts and then clamping it in position; the holes on either side of the posts are threaded so that the sample can be clamped firmly to the stage. The geometry of the samples used is shown in Fig. 5. Typical sample dimensions are $0.01 \times 0.003 \times 0.000125$ m, although the length of the sample can be reduced to 0.007 m. The holes at either end are machined into the sample prior to the final anneal and the central region electropolished using conventional solutions in a modified holder for a twin jet polisher. Numerous materials, including Fe [22,23], Ni [24], Ni-S alloy [28], Al [26], Al-alloys [25], Ni_3Al [29], Ti [27] Ti-alloys [31,32], 316 stainless steel [30], IN-903 [33], FeAl and Fe_3Al [34] have been deformed in-situ in the environmental cell TEM. A surprising feature of these studies is that the effect of hydrogen on the mobility of dislocations is independent of crystal structure and is the same for edge, screw, mixed, and partial dislocations. Therefore, in the following section examples from different materials are used to illustrate the salient features.

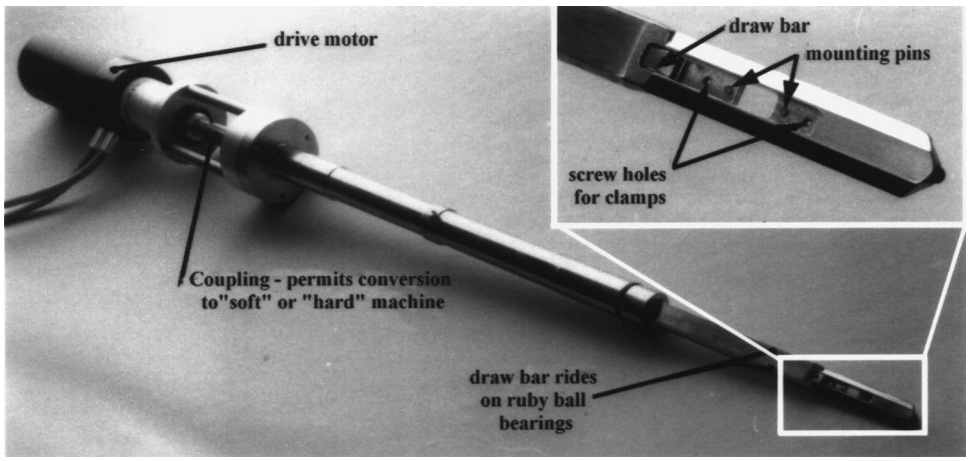

Fig. 4. Straining stage for a transmission electron microscope.

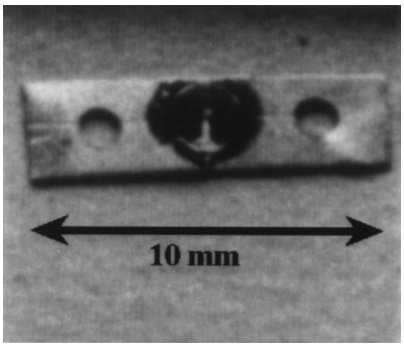

Fig. 5. Geometry of the samples used in the in-situ TEM deformation experiments.

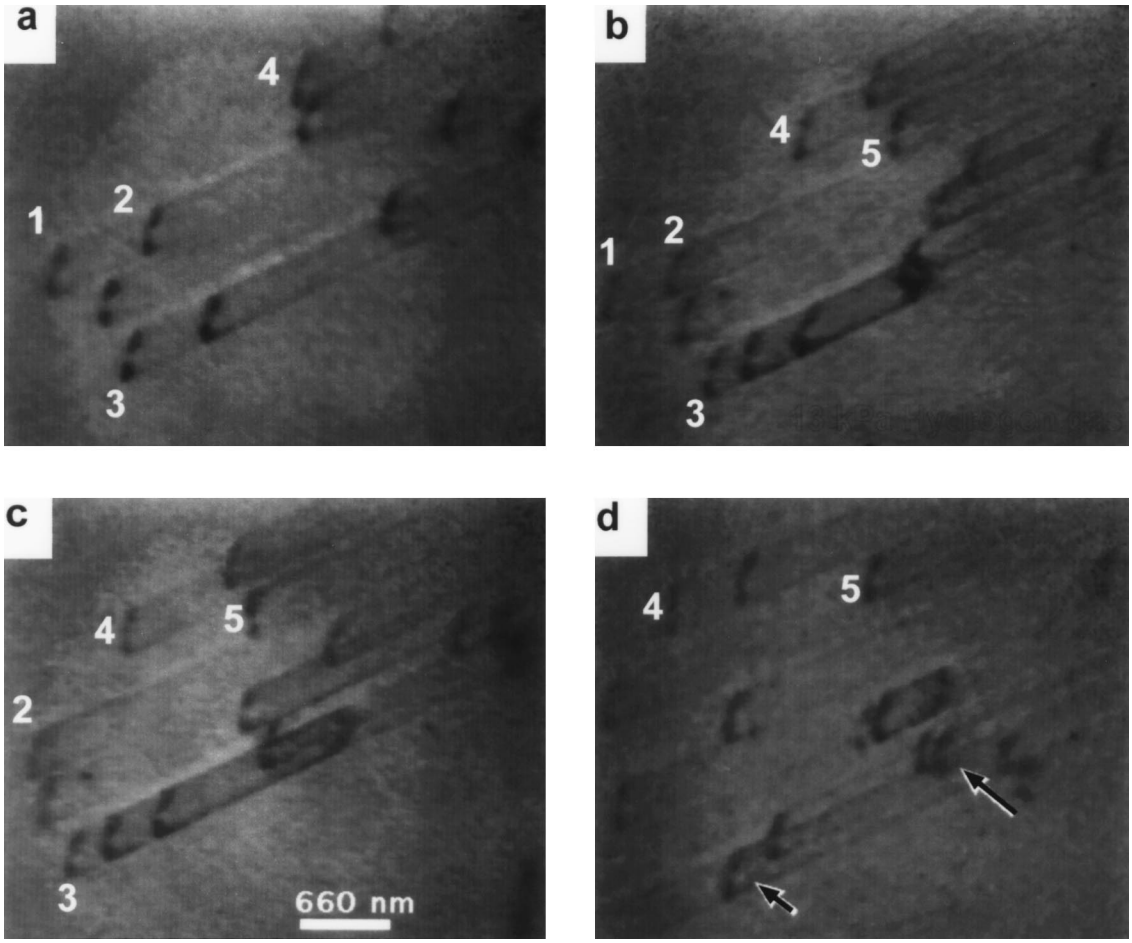

Fig. 6. The effect of hydrogen on the mobility of dislocations in α-Ti [27]. The numbers identify the same dislocation in successive images and the arrows indicate new dislocations that have appeared in the field of view. Conditions are: (a) vacuum; (b); (c); and (d) 100 torr of hydrogen gas.

3.1. Effect of hydrogen on dislocation mobility

The series of images presented in Fig. 6 shows the effect of hydrogen on the mobility of dislocations in α-Ti [27]. The arrangement of dislocations produced by deforming the sample in vacuum is shown in Fig. 6(a). During the introduction of hydrogen gas, the stage displacement was held constant. The dislocation motion induced by the introduction of hydrogen gas (gas pressure 100 torr) can be seen by comparing the positions of dislocations 1–5 in Fig. 6(b)–(d). New dislocations also appear in the field of view, some examples are marked by arrows in Fig. 6(d). If the gas is removed from the cell, the dislocations stop moving. Reintroduction of the gas causes the dislocations to move again. The effect of hydrogen on the dislocation velocity is quantified in Fig. 7, in which the ratio of the dislocation velocity in a hydrogen environment to that in vacuum is plotted as a function of hydrogen pressure. The dislocation velocity increases in the presence of hydrogen, and with increasing hydrogen pressure. Curve 2 in Fig. 7 shows the effect of removing and reintroducing hydrogen on the dislocation velocity. Reintroducing hydrogen gas causes the dislocations to start moving and their velocity to increase although a higher hydrogen gas pressure is now required.

Within the framework of the hydrogen-shielding model, the separation distance between dislocations in a pileup should decrease when hydrogen is introduced. An example of solute hydrogen causing a decrease in the separation distance between dislocations in a pileup in 310s stainless steel is presented in Fig. 8 [42]. The initial dislocation configuration was created by deforming the sample in vacuum, Fig. 8(a). Hydrogen gas was introduced to the system and as the gas pressure increased the dislocations moved closer to the grain boundary and the separation distance between the dislocations decreased. The overall shift in position of the dislocations is more evident in Fig. 8(f), which was formed by superimposing a negative image (white dislocations) of Fig. 8(e) on a positive image of Fig. 8(a). Clearly, all of the dislocations have moved closer to the barrier and the distance between the dislocations has decreased.

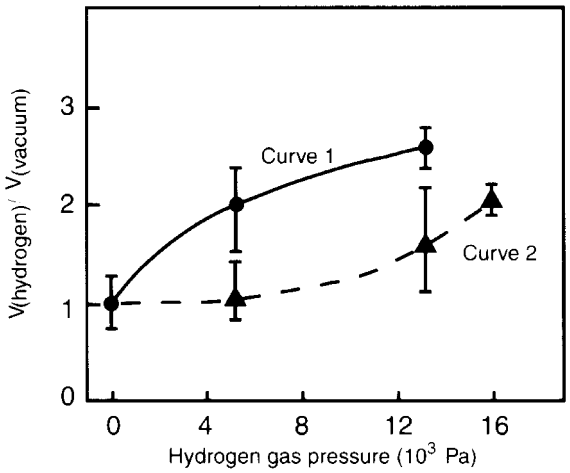

Fig. 7. Ratio of the dislocation velocity in a hydrogen environment to that in vacuum as a function of hydrogen pressure [27]. Curve 1 shows the effect of introducing hydrogen the first time and curve 2 the effect after hydrogen has been removed and reintroduced.

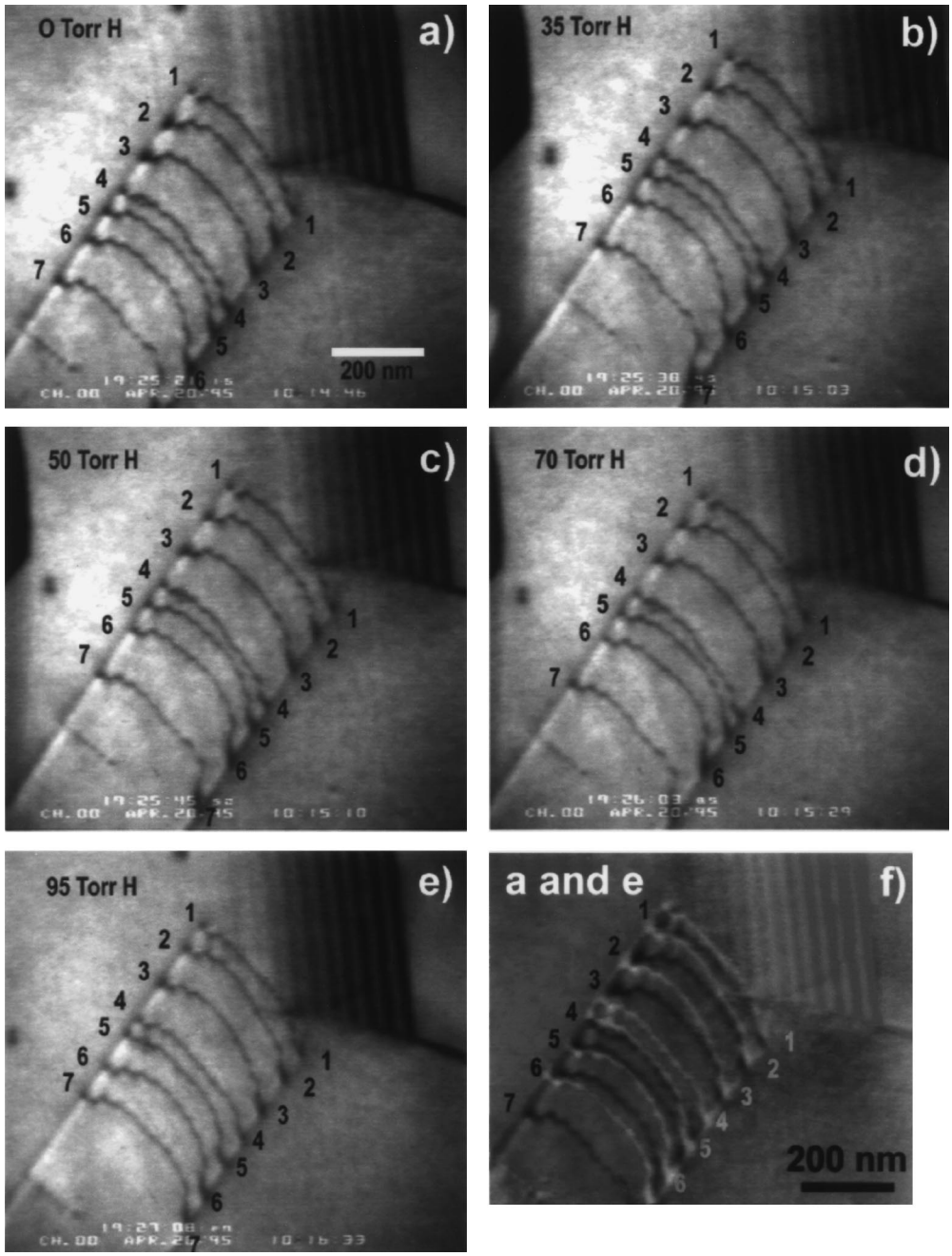

Fig. 8. Reduction of the separation distance between dislocations in a pileup in 310s stainless steel due to solute hydrogen [42]. The hydrogen gas pressures are indicated. Image f is a composite image made from a positive of image a (black dislocations) and a negative of image e (white dislocations).

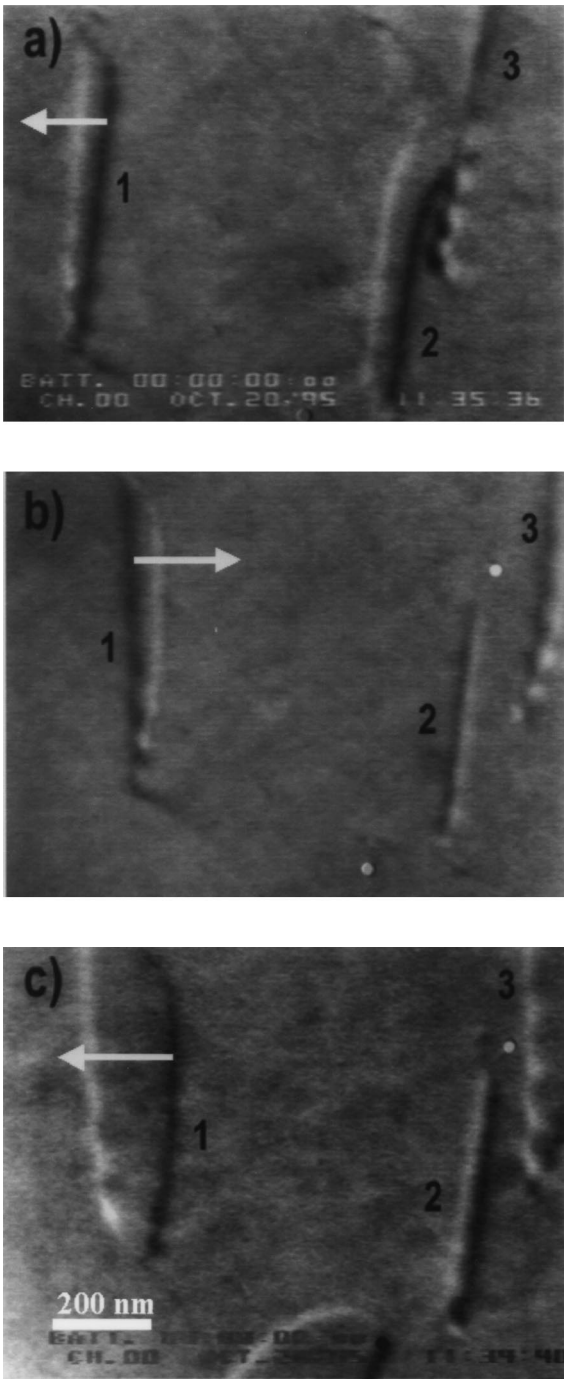

Fig. 9. Reversal of the direction of motion of dislocations on adding and removing hydrogen from high-purity aluminum. These are composite images formed by superimposing a positive image (black) showing the initial position of the dislocation on a negative image (white) showing the final position. (a) Hydrogen pressure is increased from 15 to 75 torr, (b) decreased from 75 to 9 torr, and (c) increased from 9 to 75 torr [42].

Removing hydrogen gas from a material eliminates the deleterious effect of hydrogen on the mechanical properties. In terms of the dislocation experiments, removing the hydrogen gas from the metal should cause the direction of motion of the dislocations to reverse and the separation distance between dislocations in a pileup to increase. On removing hydrogen from 310s stainless steel the dislocations in the pileup in Fig. 8(e) did not move but remained locked in position. Ferreira [42] attributed the lack of reversibility to solute pinning, arguing that the force created when hydrogen is removed is not sufficient to overcome solute pinning effects and, hence, the dislocations are locked in position. The situation was different in high-purity aluminum in which the impurity level was significantly lower than in the steel. The direction of dislocation motion was reversed when hydrogen was added and removed. A series of composite images showing this effect is presented in Fig. 9. In each image the black dislocation shows the position of the dislocation prior to the indicated change in gas pressure and the white dislocation the position afterwards. In Fig. 9(a), the hydrogen pressure was increased from 15 to 75 torr and dislocations 1 and 2 moved toward the left. Decreasing the hydrogen pressure from 75 to 9 torr caused these dislocations to move in the opposite direction, Fig. 9(b). Fig. 9(c) shows that the direction can be changed by again increasing the pressure of gas from 9 to 75 torr.

From observations of slip lines, it has been shown that there is a tendency for solute hydrogen to enhance strain localization [43–51] and slip planarity although this may be restricted to the near surface [46,52–54]. An example of increased slip localization in 310s stainless steel is shown in Fig. 10, which compares the side surfaces of hydrogen-free and hydrogen-charged samples deformed at 295 K and at a strain rate of 5.5×10^{-5} s^{-1} [50]. With increasing hydrogen content the slip lines become coarser and straighter, and the slip steps higher. Abraham and Altstetter [50] deformed a sample containing 9.2 at. pct hydrogen to just beyond the yield point discontinuity and found that slip planarity and slip localization were still enhanced, showing that in this case slip localization was not simply due to large strains. Slip localization accompanied by an increase in the flow stress has also been reported in Ni [55], a nickel-base single crystal γ/γ' superalloy [45], and ferritic alloys [56]. In contrast slip localization along with a decrease in the flow stress has been reported in Al [57].

To account for slip localization accompanied by either hardening or softening, Birnbaum

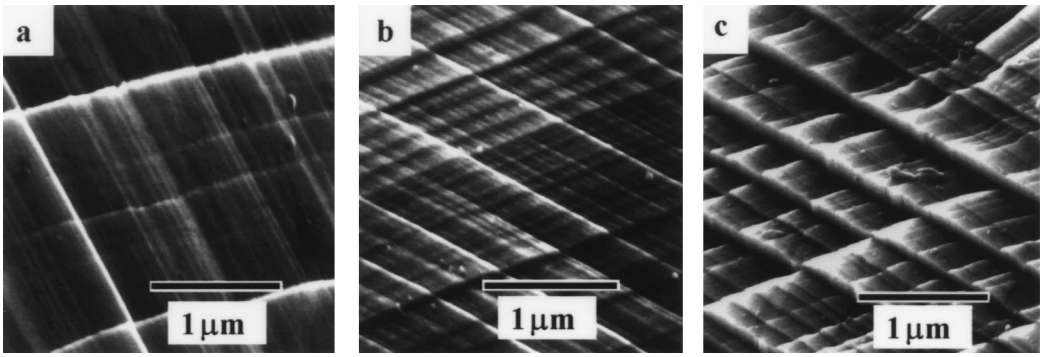

Fig. 10. Effect of hydrogen on slip localization in 310 s stainless steel (a) uncharged, (b) 0.18 at pct H and (c) 2.7 at pct H [50].

[58] proposed that the ratio of flow stress for a specimen undergoing slip localization (τ_l) to one in which deformation is occurring homogeneously (τ_u) can be expressed as

$$\frac{\tau_l}{\tau_u} = \left(\frac{l_u}{l_l}\right)^{1/m} \tag{3}$$

where the ratio l_l/l_u is the fraction of the gauge length over which slip is localized, and m is a material dependent term with a value between 1 and 30. This ratio is approximately equal to the ratio of the slip line density in the region in which slip localization occurs to that in the region exhibiting uniform slip. Where slip localization occurs there will be a reduction in the effective gauge length, the effective dislocation density, and a necessary increase in the dislocation velocity to maintain the imposed strain rate. As the dislocation velocity is related to the stress by a power-law relationship, an increase in velocity will be accompanied by an increase in flow stress.

The ratio of the flow stress in the presence of hydrogen and flow localization, $\tau_{H,l}$, to the measured flow stress, τ, can be expressed as

$$\frac{\tau_{H,\,l}}{\tau} = \left(\frac{\tau_l}{\tau_u}\right)\left(\frac{\tau_H}{\tau}\right) = \left(\frac{l_u}{l_l}\right)^{1/m}\left[\frac{(\rho_m K_o)^{1/m}}{(\rho_{m,\,H} K_{o,\,H})^{1/m_H}}\right]. \tag{4}$$

In Eq. (4), ρ_m is the density of mobile dislocations, K_o is a constant relating the mean dislocation velocity to the shear stress raised to the power m, and the subscript H indicates the presence of hydrogen. The dependence of these parameters on hydrogen concentration has not been determined. An increase or decrease in the measured flow stress will be determined by the effect of hydrogen on slip localization (τ_l/τ_u) and on the dislocation mobility (τ_H/τ). From the in-situ TEM experiments it is known that the generation rate and mobility of dislocations are increased in a hydrogen environment. It is then reasonable to assume that $K_{o,H}$ and m_H will also be increased in a hydrogen environment [58]. The conditions for microscopic softening and hydrogen can then be expressed as

$$\left(\frac{l_u}{l_l}\right) > \left(\frac{[\rho_{m,\,H} K_{o,\,H}]^{m/m_H}}{\rho_m v_o}\right) \text{ for hardening}$$

$$\left(\frac{l_u}{l_l}\right) < \left(\frac{[\rho_{m,\,H} K_{o,\,H}]^{m/m_H}}{\rho_m v_o}\right) \text{ for softening.} \tag{5}$$

Thus slip localization can occur when hydrogen reduces the barriers to dislocation motion because of the inhomogeneous distribution of hydrogen. Alternatively if hydrogen causes hardening, slip localization can occur if the deformation reduces the stress for further slip. This process may occur at lower levels of stress if hydrogen also enhances the dislocation mobility.

Ulmer and Altstetter [47] have suggested that slip localization in the presence of hydrogen is due to hydrogen atmospheres locking and immobilizing dislocations and to hydrogen activating dislocation sources to produce new mobile dislocations with a predominantly edge

character. As these new dislocations do not cross-slip, the slip bands will become narrower. No direct evidence for hydrogen affecting the character of dislocations was, however, presented.

Ferreira et al. [59] have provided the first direct experimental evidence that hydrogen can inhibit cross-slip in high-purity Al by stabilizing the edge component of mixed dislocations. The series of images presented in Fig. 11 shows hydrogen-locking dislocations in the midst of the cross-slip process. Initially the dislocations are moving in the direction indicated by the arrows labeled 1. The line direction of a portion of the dislocation changes, corresponding to this segment having cross-slipped and started to move on the cross-slip plane as indicated by arrow 2. This change in direction is perhaps more apparent in the comparison image of Fig. 11(g), in which a negative (white dislocations) of image 11(c) is superimposed on a positive image of 11(b). At higher hydrogen pressures, the cross-slip process can be stopped with part of the dislocation residing on the cross-slip plane and part on the primary slip plane. This can be seen by comparing Fig. 11(c) and (d), which show the effect of holding the gas pressure constant at 85 torr for 27 s on the position of the dislocations. That no motion of the dislocations occurs in this time is easier to see in the comparison image of Fig. 11(h) in which

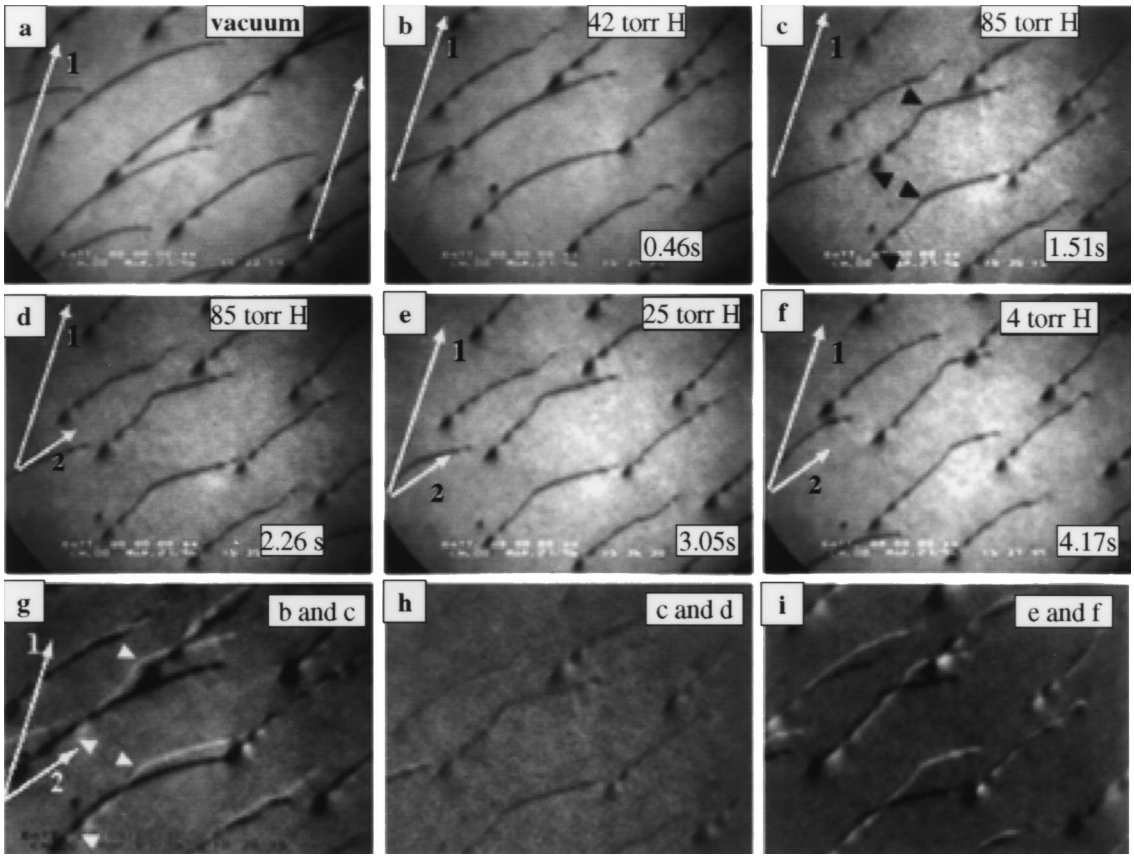

Fig. 11. Effect of hydrogen on the process of cross slip. (a) Dislocation motion in vacuum, the arrows indicate the direction of motion, (b) 42 torr of H_2, (c) 85 torr of H_2, (d) 85 torr of H_2, (e) 25 torr of H_2, and (f) 4 torr of H_2. (g)–(i) Comparison of images b and c, c and d, and e and f [59].

(c) and (d) are compared. The weak contrast of Fig. 11(h) shows that in this time interval the dislocations have not changed their position. Cross slip continues (Fig. 11(e),(f) and (i)) as the hydrogen pressure is reduced. This effect of hydrogen has only been observed in high-purity Al, but it does provide direct evidence for hydrogen influencing the character of the dislocation and provides a mechanism by which hydrogen can cause an increase in slip planarity.

To explain how solute hydrogen locked the dislocations in the process of cross slip, Ferreira et al. [59] considered the effect of a hydrogen atmosphere on the energy of an edge dislocation, and the size of the atmosphere formed on an edge and a screw dislocation. Calculations of the self-energy of the edge dislocation-hydrogen complex showed that it is lower than that of an edge dislocation although not as low as that of a screw dislocation. In addition the atmosphere associated with an edge dislocation will be more substantial than around a screw dislocation. Therefore, before an edge segment can reorient to the screw geometry needed for cross-slip, the atmosphere will have to be returned to solution, which will increase the total system energy. The reduction of the energy of the edge dislocation with a hydrogen atmosphere and the difficulty in removing the atmosphere from the edge dislocation will tend to favor the edge over the screw configuration. Consequently, the attraction of solute hydrogen to edge character dislocation segments will prohibit cross-slip and will increase slip planarity.

Observations of increased slip planarity due to solute hydrogen were initially explained by hydrogen reducing the stacking-fault energy of the material. A reduction in the stacking-fault energy would allow for greater separation between partial dislocations and, hence, a greater force would be needed to form the constriction necessary for cross-slip. The stacking-fault energy can be determined from the separation distance between the partial dislocations involved in a dislocation node. Fig. 12 shows examples of weak-beam dark-field images of dislocation nodes produced in 310s stainless steel by deforming some samples in vacuum and others in a gaseous hydrogen atmosphere. After correcting for the differences in imaging

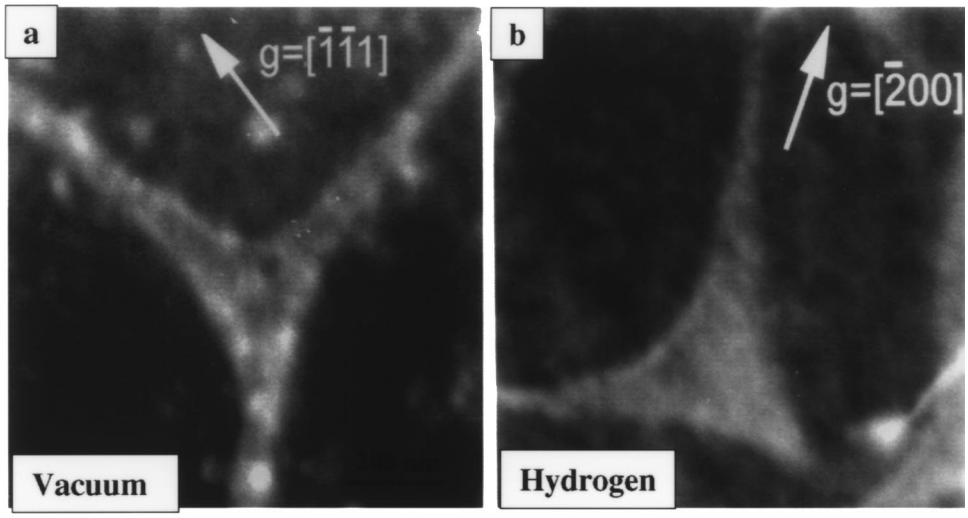

Fig. 12. Weak-beam dark-field images of dislocation nodes produced in 310s stainless steel by deformation in (a) vacuum and (b) a hydrogen environment [65].

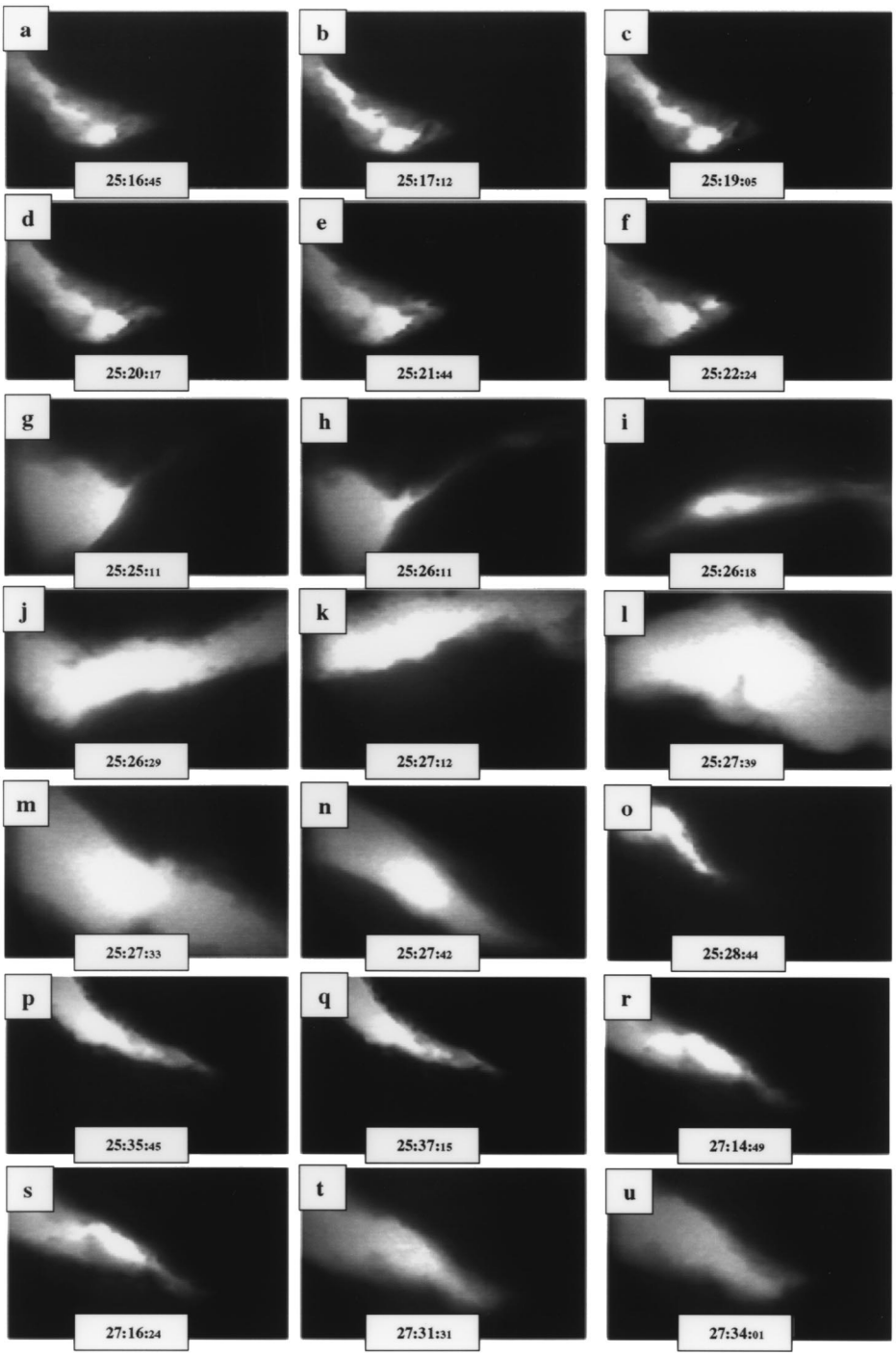

Fig. 13. Propagation of a static crack in Fe due to an increase in the hydrogen gas pressure [22]. (a)–(o) 100 torr of hydrogen, (p) and (q) vacuum and (r)–(u) 250 – 300 torr of hydrogen.

conditions, the orientation of the nodes with respect to foil normal, and the degradation in instrument resolution due to the presence of the hydrogen environment, the average value of the stacking-fault energy was found to decrease from 34.2 mJ m^{-2} in the hydrogen-free material to 27.5 mJ m^{-2} in the hydrogen-charged material. This is a decrease of about 20%. Increases in slip planarity due to hydrogen have been reported in Fe, Al and Ni, which have stacking-fault energies of ~900 mJ m^{-2}, 166 mJ m^{-2} [60], and 120–130 mJ m^{-2} [61], respectively. Assuming that the magnitude of the hydrogen-induced reduction in the stacking-fault energy is of the order of 20% in these materials, this will not be sufficient to increase the separation distance between partial dislocations to an extent where cross-slip will be affected.

3.2. Effect of hydrogen on crack propagation

The experimental observations described above have focused on the effect of hydrogen on dislocations. Effects of hydrogen on the propagation of transgranular and intergranular cracks have also been observed during in-situ deformation experiments in the environmental cell TEM. In comparing the propagation of transgranular cracks in vacuum and gaseous hydrogen environments it was observed that similar deformation mechanisms were involved [22,24]. The primary difference in behavior was that crack advance occurred at lower stresses in a hydrogen atmosphere than in vacuum. Evidence for this is shown in Fig. 13, in which a static crack in Fe is shown to propagate simply by increasing the pressure of gas in the environmental cell. The crack was formed in vacuum and then the load held constant. Hydrogen gas (pressure = 200 torr) was leaked into the environmental cell and the crack advanced rapidly, as shown in Fig. 13(a)–(p). The gas was removed and crack propagation halted, Fig. 13(p) and (q) show no crack propagation. Hydrogen gas was then reintroduced and crack propagation occurred at some hydrogen pressure. Fig. 13(r)–(u) show crack propagation as the pressure of

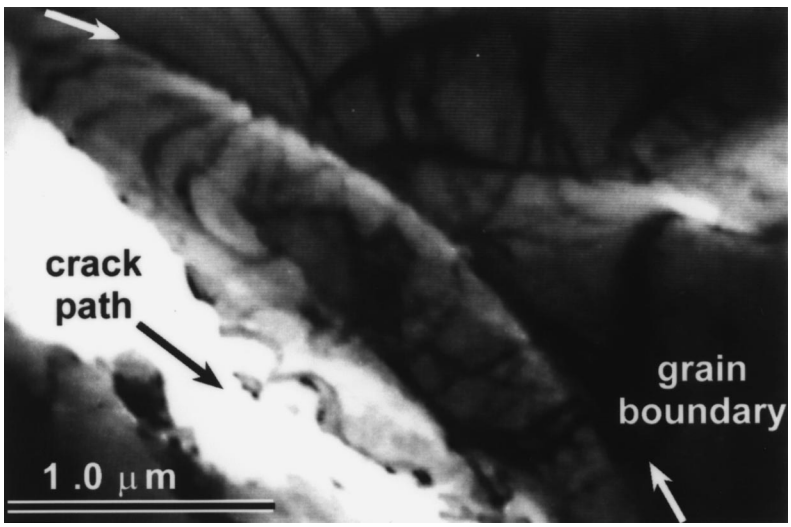

Fig. 14. "Intergranular" failure in Fe due to hydrogen. The crack propagates in the volume adjacent to, and follows the contour of, the grain boundary [22].

gas is increased from 250 to 300 torr. Crack propagation is proceeded by extensive thinning of the region ahead of the crack, indicating enhanced dislocation activity.

In some materials, the loss of ductility is accompanied by a change in fracture mode from ductile transgranular to "brittle" intergranular. In the in-situ TEM deformation experiments, two types of grain boundary failure were observed. In one case, the crack propagated in the volume close to the grain boundary but not in the plane of the grain boundary. In the other, the crack propagated in the grain boundary plane. Examples illustrating these different behaviors are compared in Figs. 14 and 15. The micrograph in Fig. 14 shows an example in Fe in which the crack follows the contour of the grain boundary but does not cause failure of the grain boundary; the arrows indicate the grain boundary. As the crack approached the grain boundary it deviated to follow the deformation band, which follows the contour of the grain boundary. Such a fracture surface when viewed macroscopically will appear intergranular. This type of grain boundary failure was a common observation in thin samples deformed in a hydrogen environment. In the absence of hydrogen, a crack approaching a grain boundary did not deviate to follow the path of the grain boundary but rather propagated through it.

In Ni-S [62] and Ni_3Al containing B [29] true intergranular fracture was observed when hydrogen was present. An example of this type of behavior is shown for a Ni-S alloy in Fig. 15. Fig. 15(b) shows schematically the situation prior to failure of the grain boundary. Several intense slip bands on two different systems can be seen. Slip bands B and E intersect the grain boundary at location C, and slip band F has penetrated through the grain boundary. On adding hydrogen and continuing the deformation, the crack progressed along slip band E but

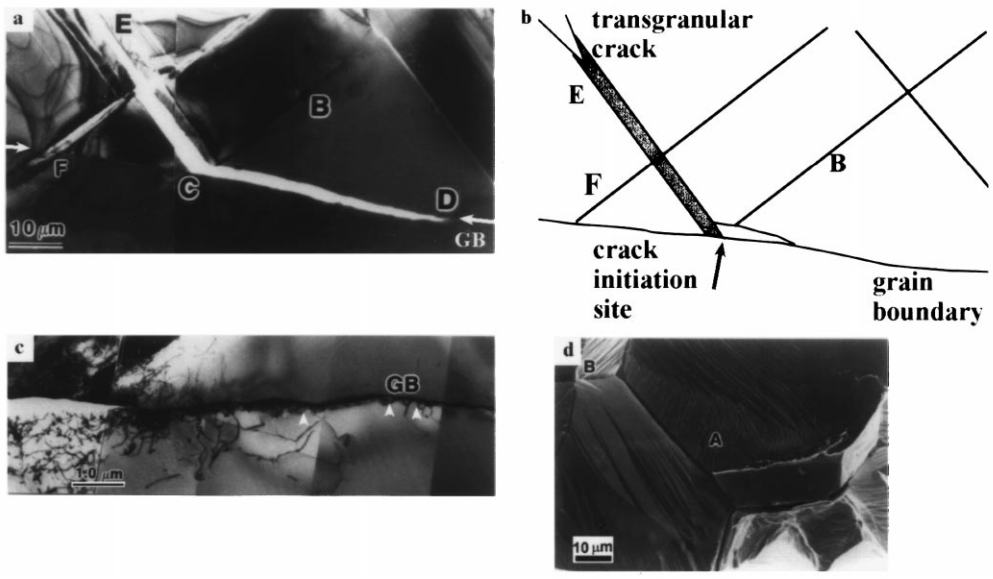

Fig. 15. Intergranular failure in a Ni-S alloy due to hydrogen. (a) Bright-field image showing intense slip bands approaching the grain boundary and cracking of the grain boundary. (b) Schematic of the reaction. (c) grain boundary failure. (d) Fractograph of the fracture surface. Arrows indicate the grain boundary and arrowheads the active dislocation sources on the grain boundary [28].

then deviated onto the grain boundary (marked by white arrows) rather then pass through it, Fig. 15(c). As shown in Fig. 15(a) the crack propagated along the grain boundary. This process involved the emission of dislocations from the crack tip and from regions of the grain boundary ahead of the advancing crack. (Examples of dislocation half-loops emerging from the grain boundary are indicated by arrowheads in Fig. 15(c).) The fracture surface is shown in the SEM image in Fig. 15(d), which confirms that the failure in the thin tensile sample was intergranular in nature. Therefore, although intergranular failure occurs, dislocations are involved in the nucleation and propagation of the crack. These observations are consistent with studies of the fracture surface morphology of Ni-S alloys with varying levels of sulfur segregated to the grain boundary and containing hydrogen [63]. The concentration of hydrogen needed to cause intergranular fracture was lower if sulfur was segregated to the grain boundaries.

3.3. Summary of in-situ TEM observations

The in-situ deformation experiments in an environmental cell TEM have provided direct evidence that hydrogen can

1. cause an increase in the velocity of edge, screw, partial and perfect dislocations in a range of materials with different crystal structures; FCC [16,24,28–30,62,64], BCC [22,23] and HCP [27];
2. cause a stationary crack to propagate by increasing the hydrogen pressure;
3. cause cracks to follow the contour of the grain boundary but not propagate in the grain boundary. In other systems, hydrogen causes grain boundary failure [29,62];
4. reduce the stacking-fault energy, the magnitude of the reduction is of the order of 20% in 310s stainless steel [65];
5. stabilize the edge component of a dislocation, and therefore prohibit cross slip [59].

A criticism often raised about these in-situ TEM experiments is that they are made in electron transparent foils, which are typically less than 200 nm thick. The proximity of the free surface will influence the behavior of dislocations. For example, the force on a straight dislocation inclined to a free surface will cause it to rotate toward the screw orientation as the surface is approached; this will cause the separation of partial dislocations to be different at the surface than in the bulk. The surface force will cause loss of glissile dislocations to the foil surface, will lower the applied stress required for the operation of near surface dislocation sources, and will influence the type of dislocation responsible for carrying the strain. However, with these caveats in mind the in-situ deformation experiments can provide insight to dislocation dynamics and how they are influenced by solute hydrogen. In addition, the current experiments are comparative in nature and changes in dislocation behavior can be attributed to the introduction of hydrogen to the sample. There is also an increasing body of evidence from studies using bulk samples that hydrogen influences the mobility of dislocations [32,35,50,51,66–69] and these are briefly described in section 4.

4. Solute hydrogen effects on plastic processes in bulk samples

In the original work by Beachem [14], it was the observation of tear ridges and dimples on fracture surfaces that led him to propose that hydrogen was unlocking rather than locking dislocations. Since then numerous examples have been presented in the literature that show evidence of plasticity on "brittle" fracture surfaces [32,51,70]. In addition to this indirect evidence, there is more direct evidence for hydrogen influencing the mobility of dislocations. For example, solute hydrogen has been reported to cause a decrease in flow stress, an increase in the magnitude of the stress relaxation [35,50,71], and an increase in the magnitude of the stress change in strain rate change tests [35,50].

Matsui et al. [66–68] studied the effect of hydrogen on the mechanical properties of iron as a function of purity. Hydrogen was introduced cathodically at low charging current densities to avoid causing surface damage and producing dislocations. They found that internal hydrogen causes either softening or hardening depending on material purity, test temperature, and strain rate. In high-purity iron, softening was observed in the temperature range from 200 to 300 K and hardening below 190 K. In the transition regime, serrated flow was observed, indicating that the dislocation structures are changing and that dynamic pinning of dislocations is occurring. Pre-yield microstrain, which is attributed to edge dislocations, was not observed in hydrogen charged samples. Matsui et al. [66–68,72] attributed the softening to hydrogen reducing the energy required to nucleate double-kinks on screw dislocations, causing a decrease in the Peierls–Nabarro interactions. The hardening below 190 K was attributed to hydrogen inhibiting the mobility of edge-like kinks. Similar results were obtaining when polycrystalline samples of high-purity iron were used. The softening behavior in high-purity iron is consistent with the in-situ TEM observations [22,23] to some degree, although the in-situ experiments showed that hydrogen enhanced the mobility of edge as well as screw dislocations.

Softening has also been reported in Al [57] and Ni [55]. However, the softening behavior in Ni was attributed to the formation of surface hydrides and the subsequent injection of dislocations to accommodate the volume difference or to the injection of dislocations due to the hydrogen concentration gradient (stress gradient) established during charging [55] and not to hydrogen influencing dislocation mobility.

Part of the complexity in resolving the mechanisms responsible for hydrogen embrittlement is that completely contrasting effects are often reported in the same system. In contrast to the reports of softening there are numerous reports of solute hydrogen increasing the flow stress, i.e., hardening. Hardening has been reported in Ni [55,73], Al [74], 21-6-9 FCC stainless steel [75], 304L stainless steel [76,77], iron [78,79], mild steel [78,79], 304 stainless steel [47,80] and 310s [47,80]. These observations have been subjected to strong criticism because of the high current densities used in some cases to introduce hydrogen. Using high current densities can produce blisters on the surface and hydrogen concentration gradients, which can cause injection of dislocations, surface transformations, and surface hydrides. In the work of Kimura and Birnbaum [55] on the effects of hydrogen on the flow behavior of nickel, hardening and softening were observed depending on the charging current density, temperature and strain rate. A flow stress decrease was observed at high charging current densities, which is the opposite response to pre-charged samples in which hydrogen caused hardening. They also found that the effects were sensitive to sample thickness, with no effect of hydrogen on the flow

behavior being found in thicker samples. This result and the observation that the effect on the flow stress stopped when the charging stopped suggested that a surface effect was responsible for both hardening and softening.

Not all studies in which hydrogen was introduced cathodically used high current densities. The work of the Matsui and coworkers [66–68,72] on high-purity iron is one notable example, although in this case softening was observed. The work of Abraham and Altstetter [80] used low current densities to introduce hydrogen to 310 s stainless steel and hardening was found. This is shown in Fig. 16 in which the stress–strain curves for hydrogen-charged and hydrogen-free material are compared. The yield and the flow stress increase with increasing hydrogen content and above 5 at. pct hydrogen there is a yield point discontinuity. The macroscopic strain to failure decreases somewhat with increasing hydrogen content. Abraham and Altstetter [80] attributed the increase in flow stress to hydrogen or hydrogen clusters acting as solute hardeners, which affect only rapidly moving dislocations.

Information on the effect of hydrogen on the dislocation mobility can be obtained from stress relaxation and strain rate change tests. In stress relaxation tests the time-dependent decrease in the stress at constant temperature and displacement is determined, which provides information on the motion of dislocations over barriers. In strain rate change tests at a given temperature and plastic strain, the measured change in the stress provides information on the interaction of dislocations with solutes. In the early work of Oriani and Josephic [71], stress relaxation tests showed a greater relaxation in a medium carbon steel (AISI 1045 steel) provided that a critical hydrogen concentration was exceeded. This result was originally

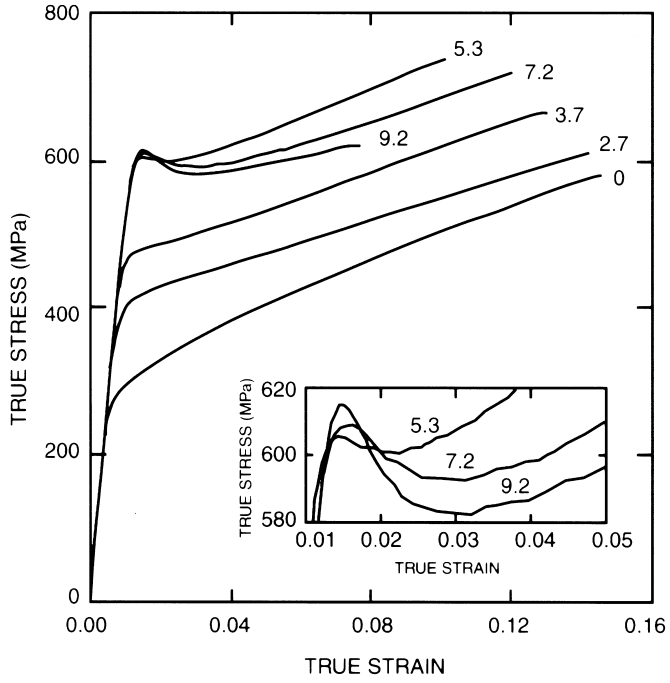

Fig. 16. Comparison of the stress–strain curves for hydrogen-charged and hydrogen-free 310s stainless steel [80].

interpreted as hydrogen-induced decohesion and decohesive growth of microvoids, which caused a decrease in internal stresses and a subsequent burst of dislocations. While hydrogen influenced microvoid nucleation and growth, it was not thought to have a direct influence on dislocation mobility. In his review article [19], Oriani suggested that the stress relaxation effect might be due to hydrogen enhancing the injection of dislocations from the sample surface, i.e., Lynch's mechanism [81,82]. The effect of hydrogen on the stress relaxation and the magnitude of the strain rate change for 310 s stainless steel are shown in Fig. 17 [50].

The stress relaxation and strain rate change test data can be related to the activation area (i.e., the area swept out during the thermally activated motion of a dislocation over a barrier) through the following expressions:

$$\left(\frac{\delta\sigma_{\mathrm{A}}}{\delta \quad \ln(t+c)}\right) = -\frac{kT}{b\Delta A}, \text{ stress relaxation case}$$

$$\left(\frac{\delta \quad \ln \quad \dot{\epsilon}}{\delta\sigma_{\mathrm{A}}}\right) = \left(\frac{\delta \quad \ln \quad \dot{\epsilon}}{\delta\sigma_{\mathrm{e}}}\right) = \frac{b\Delta A}{kT}, \text{ strain rate change case}$$

In these equations σ_{A} is the applied stress, σ_{e} is the local effective stress, $\dot{\epsilon}$ the strain rate, ΔA the activation area, and b the magnitude of the Burgers vector of the dislocations. The results of this analysis for 310 s stainless steel are shown in Table 1.

The activation area swept out by a dislocation as it moves over a barrier decreases with increasing hydrogen concentration in both types of test. A larger decrease in ΔA was found in nickel [35]. These results are consistent with hydrogen causing the dislocations to move more readily. In the case of 310 s stainless steel, Abraham and Altstetter [50] suggested that

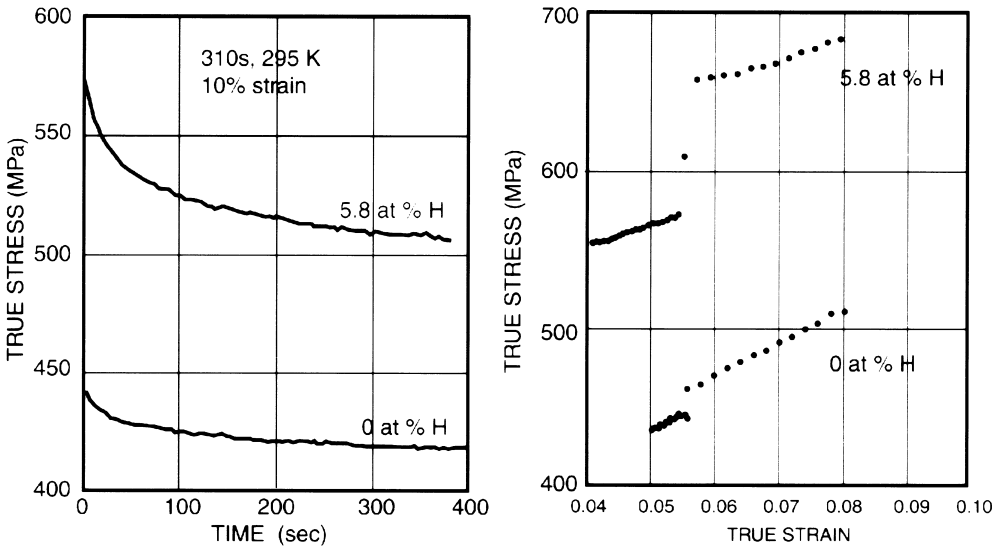

Fig. 17. The effect of hydrogen on the (a) stress relaxation and (b) the magnitude of the strain rate change for 310s stainless steel [50].

Table 1
Effect of hydrogen on the activation are from stress relaxation and strain rate change tests [50]

Hydrogen content (at.%)	Strain (%)	ΔA from stress relaxation tests	ΔA from strain rate change tests
0	6	51 b^2	
3	6	13 b^2	
5.8	6	7 b^2	
0	10		52 b^2
5.8	10		17 b^2

hydrogen influenced the mobility of slowly moving dislocations that can drag the hydrogen atmosphere along.

5. Conclusion

There is now considerable evidence, from the in-situ TEM deformation experiments in a hydrogen environment and from mechanical property tests, showing that hydrogen can enhance the mobility of dislocations. The experimental observations are in general agreement with the hydrogen-shielding model.

Acknowledgements

This work was sponsored by the Department of Energy under grant DEFG02-91-ER45349. This work would not have been possible without contributions from the graduate students and post-doctoral fellows that I have had the pleasure to work with. I would especially like to thank Professor Howard Birnbaum, without whose support, encouragement and advice much of this would not have been possible. Discussions with Professors C. J. Altstetter and Petros Sofronis and Mr D. Lillig are gratefully acknowledged.

References

[1] Johnson WH. On some remarkable changes produced in iron and steel by the action of hydrogen and acids. In: Beachem CD, editor. Proceedings of the Royal Society of London 1875, 23, (reproduced in "Hydrogen damage"). American Society for Metals, Ohio, 1977.
[2] Zapffe C. Discussion of metal arc welding of steels by S. A. Herres. Transactions, American Society for Metals 1947;39:191–2.
[3] Kazinczy Fd. A theory of hydrogen embrittlement. Journal of the Iron and Steel Institute 1954;177:85–92.
[4] Petch NJ. Delayed fracture of metals under static load. Nature 1952;169:842–3.
[5] Petch NJ. Lowering of the fracture stress due to surface adsorption. Phil Mag 1956;1:331–5.
[6] Morlet JG, Johnson HH, Troiano AR. A new concept of hydrogen embrittlement in steel. Journal of the Iron and Steel Institute 1958;189:37–41.

[7] Troiano AR. The role of hydrogen and other interstitials in the mechanical behavior of metals. Trans ASM 1960;52:54–80.
[8] Pressouyre GM, Bernstein IM. A quantitative analysis of hydrogen trapping. Metall Trans A 1978;9A:1571–80.
[9] Pressouyre GM, Bernstein IM. A kinetic trapping model for hydrogen-induced cracking. Acta Metall 1979;27:89–100.
[10] Pressouyre GM. Trap theory of hydrogen embrittlement. Acta Metall 1980;28:895–911.
[11] Williams DN. The hydrogen embrittlement of titanium alloys. J Inst Metals 1963–63;91:147–52.
[12] Windle RH, Smith GC. The effect of hydrogen on the plastic deformation of nickel single crystals. Mater Sci J 1968;2:187–91.
[13] Cornet M, Trichet MF, Talbot-Bernard S. Influence of hydrogen on plastic deformation and fracture of iron, studied by electron microscopy and Auger spectrography. Memoires Scientifiques de la Revue de Metallurgie 1977;74:307–16.
[14] Beachem CD. A new model for hydrogen-assisted cracking (hydrogen embrittlement). Metall Trans A 1972;3:437–51.
[15] Lynch SP. Mechanisms of hydrogen-assisted cracking. Met Forum 1979;2:189–200.
[16] Eastman J, Heubaum F, Matsumoto T, Birnbaum HK. The effect of hydrogen on the solid solution strengthening and softening of nickel. Acta Metall 1982;30:1579–86.
[17] Hirth JP. Effects of hydrogen on the properties of iron and steel. Metall Trans A 1980;11A:861–90.
[18] Birnbaum HK. Mechanical properties of metal hydrides. J Less-Common Met 1984;104:31–41.
[19] Oriani RA. Hydrogen-the versatile embrittler. Corrosion 1987;43:390–7.
[20] Birnbaum HK. Mechanisms of hydrogen related fracture of metals. In: Moody NR, Thompson AW, editors. Hydrogen effects on material behavior. Metals and Materials Society: The Minerals, 1990. p. 639–58.
[21] Lynch SP. Environmentally assisted cracking: overview of evidence for an adsorption-induced localised-slip process. Acta Metall 1988;36:2639–61.
[22] Tabata T, Birnbaum HK. Direct observations of hydrogen enhanced crack propagation in iron. Scr Metall 1984;18:231–6.
[23] Tabata T, Birnbaum HK. Direct observation of the effect of hydrogen on the behavior of dislocations in iron. Scripta Metall 1984;17:947–50.
[24] Robertson IM, Birnbaum HK. HVEM study of hydrogen effects on the deformation of nickel. Acta Metall 1986;34:353–66.
[25] Bond GM, Robertson IM, Birnbaum HK. The influence of hydrogen on deformation and fracture processes in high-strength aluminum alloys. Acta Metall 1987;35:2289–96.
[26] Bond GM, Robertson IM, Birnbaum HK. Effects of hydrogen on deformation and fracture processes in high-purity aluminum. Acta Metall 1988;36:2193–7.
[27] Shih DS, Robertson IM, Birnbaum HK. Hydrogen embrittlement of alpha titanium: in situ TEM studies. Acta Metall 1988;36:111–24.
[28] Lee TC, Robertson IM, Birnbaum HK. HVEM in situ deformation study of nickel doped with sulfur. Acta Metall 1989;37:407–15.
[29] Bond GM, Robertson IM, Birnbaum HK. On the mechanisms of hydrogen embrittlement of Ni_3Al alloys. Acta Metall 1989;37:1407–13.
[30] Rozenak P, Robertson IM, Birnbaum HK. HVEM studies of the effects of hydrogen on the deformation and fracture of AISI type 316 austenitic stainless steel. Acta Metall Mater 1990;38:2031–40.
[31] Xiao H. PhD thesis, University of Illinois, 1993.
[32] Teter D. PhD thesis, University of Illinois, 1996.
[33] Robertson IM, Birnbaum HK. IN-903, unpublished 1996.
[34] Lillig D, Legzdina D, Robertson IM, Birnbaum HK. 1996.
[35] Sirois E, Birnbaum HK. Effects of hydrogen and carbon on thermally activated deformation of nickel. Acta metall mater 1992;40:1377–85.
[36] Birnbaum HK, Sofronis P. Hydrogen-enhanced localized plasticity-a mechanism for hydrogen-related fracture. Mater Sci Eng A, Struct Mater, Prop Microstruct Process 1993;A176:191–202.
[37] Butler EP, Hale KF Glauert AM, editors. Practical methods in electron microscopy, vol. 9. Amsterdam: North-Holland, 1981. p. 239–308.

[38] Lee TC, Dewald DK, Eades JA, Robertson IM, Birnbaum HK. An environmental cell transmission electron microscope. Review of Scientific Instruments 1991;62:1438–44.
[39] Teter D, Ferreira P, Robertson IM, Birnbaum HK. An environmental cell TEM for studies of gas-solid interactions. In: Jones RH, Baer DR, editors. New techniques for characterizing corrosion and stress corrosion. Clevland, Ohio: TMS, Warrendale, Pa, 1995. p. 53–72.
[40] Robertson IM, Teter D. Microscopic studies on hydrogen effects on mechanical properties. Jom 1996;48:55–60.
[41] Bond GM, Robertson IM, Birnbaum HK. On the determination of the hydrogen fugacity in a cell Tem facility. Scripta Metall 1986;20:653–8.
[42] Ferreira PJ, Robertson IM, Birnbaum HK. Hydrogen effects on the interaction between dislocations. Acta Mater 1998;46:1749–57.
[43] Louthan Jr MR. Strain localization and hydrogen embrittlement. Scr Metall 1983;17:451–4.
[44] Kramer IR, Hirth JP. Effect of hydrogen on the dislocation density distribution in 1090 steel. Scr Metall 1984;18:539–41.
[45] Dollar M, Bernstein IM. The effect of hydrogen on deformation substructure, flow and fracture in a nickel-base single crystal superalloy. Acta Metall 1988;36:2369–76.
[46] Park IG, Thompson AW. Hydrogen-assisted ductile fracture in spheroidized 1520 steel. I. Axisymmetric tension. Metall Trans A, Phys Metall Mater Sci 1990;21A:465–77.
[47] Ulmer DG, Altstetter CJ. Hydrogen-induced strain localization and failure of austenitic stainless steels at high hydrogen concentrations. Acta Metall Mater 1991;39:1237–48.
[48] Le TD, Bernstein IM. Effects of hydrogen on dislocation morphology in spheroidized steel. Acta Metall Mater 1991;39:363–72.
[49] McEvily AJ, May IL. Hydrogen-assisted cracking. Mater Charact 1991;26:253–68.
[50] Abraham DP, Altstetter CJ. Hydrogen-enhanced localization of plasticity in an austenitic stainless steel. Metall Mater Trans A, Phys Metall Mater Sci 1995;26A:2859–71.
[51] Yeh MS, Huang JH. Internal hydrogen-induced subcritical crack growth in Ti-6Al-4 V. Scr Mater 1997;36:1415–21.
[52] Thompson AW. Hydrogen-assisted fracture in single-phase nickel alloys. Scr Metall 1982;16:1189–92.
[53] Walston WS, Bernstein IM, Thompson AW. The effect of internal hydrogen on a single-crystal nickel-base superalloy. Metall Trans A, Phys Metall Mater Sci 1992;23A:1313–22.
[54] Xiangyun T, Thompson AW. Hydrogen effects on slip character and ductility in Ni-Co alloys. Mater Sci Eng A, Struct Mater, Prop Microstruct Process 1994;A186:113–9.
[55] Kimura A, Birnbaum HK. Effects of H on flow stress of Ni. Acta Metall 1987;35:1077–88.
[56] Bernstein IM. Role of microstructure and the environment on dislocation behavior. In: Chu SNG, Liaw PK, Arsenault RJ, Sadananda K, Chan KS, Gerberich WW, et al., editors. Micromechanics of advanced materials. Symposium in honor of Professors James C. M. Li's 70th Birthday. Proceedings, 1995. p. 401–6.
[57] Zeides F. PhD thesis, University of Illinois, 1986.
[58] Birnbaum HK. Hydrogen effects on deformation-relation between dislocation behavior and the macroscopic stress–strain behavior. Scr Metall Mater 1994;31:149–53.
[59] Ferreira PJ, Robertson IM, Birnbaum HK. Accepted for publication, Acta Mater. 1999.
[60] Murr LE. Interfacial phenomena in metals and alloys. Reading, MA: Addison-Wesley, 1975.
[61] Carter CB, Holmes SM. The stacking-fault energy of nickel. Phil Mag 1977;35:1161–72.
[62] Lee TC, Robertson IM, Birnbaum HK. An HVEM in-situ deformation study of nickel doped with sulfur. Acta Metall 1989;37:407–15.
[63] Lassila DH, Birnbaum HK. Intergranular fracture of nickel: the effect of hydrogen-sulphur co-segregation. Acta Metall 1987;35:1815–22.
[64] Hanninen HE, Lee TC, Robertson IM, Birnbaum HK. In situ observations on effects of hydrogen on deformation and fracture of A533B pressure vessel steel. Journal of Materials Engineering & Performance 1993;2:807–18.
[65] Ferreira PJ, Robertson IM, Birnbaum HK. Influence of hydrogen on the stacking-fault energy of an austenitic stainless steel. Materials Science Forum 1996;207(209):93–6.
[66] Matsui H, Kimura H, Moriya S. The effect of hydrogen on the mechanical properties of high purity iron. I.

Softening and hardening of high purity iron by hydrogen charging tensile deformation. Mater Sci Engng 1979;40:207–16.
[67] Moriya SMHKH. The effect of hydrogen on the mechanical properties of high purity iron. II. Effect of quenched-in hydrogen below room temperature. Mater Sci Engng 1979;40:217–25.
[68] Matsui H, Kimura H, Kimura A. The effect of hydrogen on the mechanical properties of high purity iron. III. The dependence of softening on specimen size and charging current density. Mater Sci Engng 1979;40:227–34.
[69] Kimura H, Matsui H. Mechanism of hydrogen-induced softening and hardening in iron. Scr Metall 1987;21:319–24.
[70] Ulmer DG, Altstetter CJ. Mechanism for hydrogen embrittlement of austenitic stainless steels. In: Moody NR, Thompson AW, editors. Hydrogen effects on material behavior. Metals and Materials Society: The Minerals, 1990. p. 421–30.
[71] Oriani RA, Josephic PH. Hydrogen-enhanced load relaxation in a deformed medium carbon steel. Acta Metall 1979;27:997–1005.
[72] Kimura H, Matsui H. Mechanisms of hydrogen-induced softening and hardening in iron. Scripta Metall 1987;21:319–24.
[73] Boniszewski T, Smith CG. The influence of hydrogen on the plastic deformation ductility and fracture of nickel in tension. Acta Metall 1963;11:165–78.
[74] Watson JW, Shen Y, Meshii M. Effect of cathodic charging on the mechanical properties of aluminum. Metallurgical Transactions A-Physical Metallurgy & Materials Science 1988;19A:2299–304.
[75] West AJ, Louthan J. Dislocation transport and hydrogen embrittlement. Metall Trans A 1982;13A:2049–58.
[76] Caskey GR. Effect of hydrogen on work hardening of Type 304L austenitic stainless steel. Scripta Metall 1981;15:1183–6.
[77] Holbrook JH, West AJ. Effect of temperature and strain rate on the tensile properties of hydrogen charged 304L, 21-6-9, and JBK 75. In: Bernstein IM, Thompson AW, editors. Hydrogen effects in metals. New York: TMS-AIME, 1981. p. 655–63.
[78] Asano S, Otsuka R. The lattice hardening due to dissolved hydrogen in iron and steel. Scripta Metall 1976;10:1015–20.
[79] Asano S, Otsuka R. Further discussion on the lattice hardening due to dissolved hydrogen in iron and steel. Scripta Metall 1978;12:287–8.
[80] Abraham DP, Altstetter CJ. The effect of hydrogen on the yield and flow stress of an austenitic stainless steel. Metall Mater Trans A, Phys Metall Mater Sci 1995;26A:2849–58.
[81] Lynch SP. Hydrogen embrittlement and liquid-metal embrittlement in nickel single crystals. Scr Metall 1979;13:1051–6.
[82] Lynch SP. A fractographic study of hydrogen-assisted cracking and liquid-metal embrittlement in nickel. J Mater Sci 1986;21:692–704.